

Geodetic Coils on Deformed Sphere

V. L. Golo^{1*} and D. O. Sinitsyn¹
¹ *Department of Mechanics and Mathematics*
Moscow University
Moscow 119 899 GSP-2, Russia

(Dated: July, 8, 2005)

We study geodetic lines on a surface generated by a small deformation of the standard 2D-sphere. We construct an auxiliary hamiltonian system with the view of describing geodetic coils and almost closed geodesics, by using the fact that loops of the coil can be well approximated by great circles of the sphere. The phase space of the auxiliary system is determined by the graph generated by separatrices of its solutions, the vertices of the graph corresponding to almost closed geodesics and the edges to the geodetic coils joining them. Topological types of the graph depend on the parameters determining the deformation. Using the method of averaging in conjunction with the computer modelling of the auxiliary system, we obtain a fairly detailed visualization of geodesics on the deformed sphere.

PACS numbers: 1111

Keywords: geodetic lines, averaging method, separatrixe

I. GEODETIC COILS

Geodesic lines on a surface can be considered either as straight lines with respect to a Riemann metric, or trajectories of a particle of mass m moving freely on the surface. The second approach allows for using the methods of analytical mechanics, and has drawn considerable attention, [1]. It should be noted that the general solution of the problem of geodetic lines is known only for certain special cases, e.g. ellipsoid, [1], [2], and the topology, or analysis situs, of

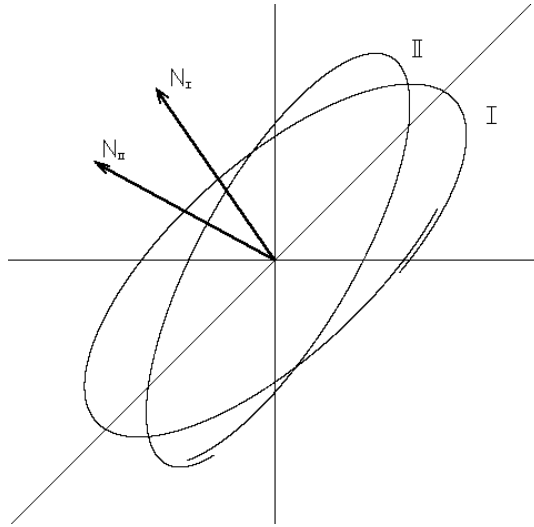


FIG. 1: Two coils I, II of a geodesic on ellipsoid; vectors N_I and N_{II} are the normals to the planes of great circles approximating the coils

*Electronic address: golo@mech.math.msu.su

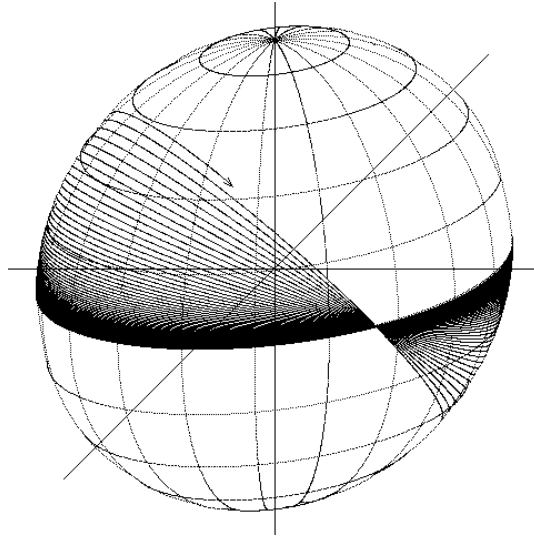


FIG. 2: Ellipsoid with main axes 1.01, 1.02, 1.03; the geodesic, corresponding to a separatrix of the auxiliary system, leaves a saddle point; the initial point $(-0.0117, 0.0001, -1.0299)$; the initial velocity $(-1.9416, 0.0194, 0.0228)$.

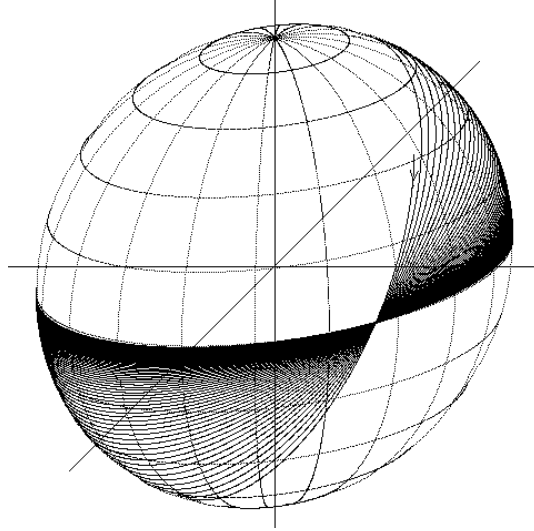


FIG. 3: Ellipsoid with main axes 1.01, 1.02, 1.03; the geodesic, corresponding to a separatrix of the auxiliary system, arrives at a saddle point; the initial point $(0.7416, 0.6169, 0.3176)$; the initial velocity $(0.4728, -1.2782, 1.3832)$

geodesics on a surface needs specific studying. In this paper we use asymptotic methods and in particular focus our attention on geodetic lines that are closed to within the first order of perturbation theory.

The central idea relies on the circumstance that in case of an ellipsoid not differing substantially from a sphere, the great circles of the latter may serve a good approximation to the ellipsoid's geodesics, if they are short enough, and one can visualize the geodesics as winding up in coils; loops or rings of the coil corresponding to great circles of the sphere, see FIG.1. Hence approximating the successive rings by great circles, we may describe the change in the position of the rings by the motion of a great circle, see FIG.1, which in its turn is determined by the normal vector \vec{L} of the plane cutting the sphere along the great circle. To cast this picture in a more quantitative form we may use the fact that the normal vector \vec{L} is the angular momentum of the particle moving along the geodetic line. This, we obtain the advantage of allowing for the use of asymptotic methods, in particular the averaging. Our main instrument is an auxiliary hamiltonian system describing the asymptotic motion of \vec{L} . It can be easily solved, so that its stationary solutions correspond to closed planar geodesics within the limit of precision provided by the averaging method ,

see FIG.2. We can get some insight into the behaviour of geodesics by considering solutions joining the stationary solutions, that is separatrixes, which, from a purely geometrical point of view, are a kind of bridges between closed geodesics. In the case of two dimensional torus in three dimensional space this phenomenon had been observed by Yu.S.Volkov, [4]. Generally, a separatrix geodesic coil does not coincide anywhere with a closed geodesic but comes infinitely close to it, and thus resembles a limit cycle, see FIG.2. The set of stationary points and separatrixes of the auxiliary system forms a net, or graph, which, as is shown in Section II can be realized on projective plane. Thus, we obtain a topological classification of geodesic coils, and find that the number of their topological types is finite.

These arguments are valid even for surfaces having a more general form than that of the ellipsoid. Studying the specific case of the deformation determined by fourth order terms involves the surface being substantially different from the ellipsoid as regards its differential geometry, as well as the algebraic structure of its equations, and hence we come across considerable difficulties by attempting a direct investigation of the geodesics. The asymptotic approach outlined above has the advantage of getting round this problem.

II. AVERAGED EQUATIONS OF GEODESICS

The equations determining geodesics on a surface can be cast in the form of the equation, [3],

$$\ddot{\vec{x}} = \lambda \frac{\partial \varphi}{\partial \vec{x}}, \quad (1)$$

where $\varphi(\vec{x})$ is the right-hand side of the constraint $\varphi(\vec{x}) = 0$ determining the surface. The Lagrangian multiplier can be found explicitly, so that the equation of motion, in the form that does not involve λ , reads

$$\ddot{\vec{x}} = - \frac{\dot{\vec{x}} \cdot \frac{\partial^2 \varphi}{\partial \vec{x}^2} \cdot \dot{\vec{x}}}{\left(\frac{\partial \varphi}{\partial \vec{x}} \right)^2} \frac{\partial \varphi}{\partial \vec{x}}. \quad (2)$$

In this paper we consider surfaces that do not differ substantially from sphere, and in assume that their equations be of the form

$$\varphi(\vec{x}) = \sum_i (x_i^2 + \varepsilon_i x_i^4) - 1.$$

where ε_i are small. Then equations (2) read

$$\ddot{x}_i = - \frac{\sum_j (2 + 12\varepsilon_j x_j^2) \dot{x}_j^2}{\sum_j (2x_j + 4\varepsilon_j x_j^3)^2} (2x_i + 4\varepsilon_i x_i^3). \quad (3)$$

The equations given above are more tractable than the usual ones employing the Christoffel symbols and an explicit parametrization of sphere, so that one may prefer them for the needs of numerical simulation, as is done in this paper. With the view of obtaining a qualitative description of geodesics, we shall consider the angular momentum

$$\vec{L} = \vec{r} \times \vec{p},$$

Its components satisfy the equations, which follow from (3)

$$\begin{aligned}
\dot{L}_1 &= -4 \frac{\sum_j (2 + 12\varepsilon_j x_j^2) \dot{x}_j^2}{\sum_j (2x_j + 4\varepsilon_j x_j^3)^2} x_2 x_3 (\varepsilon_3 x_3^2 - \varepsilon_2 x_2^2) \\
\dot{L}_2 &= -4 \frac{\sum_j (2 + 12\varepsilon_j x_j^2) \dot{x}_j^2}{\sum_j (2x_j + 4\varepsilon_j x_j^3)^2} x_3 x_1 (\varepsilon_1 x_1^2 - \varepsilon_3 x_3^2) \\
\dot{L}_3 &= -4 \frac{\sum_j (2 + 12\varepsilon_j x_j^2) \dot{x}_j^2}{\sum_j (2x_j + 4\varepsilon_j x_j^3)^2} x_1 x_2 (\varepsilon_2 x_2^2 - \varepsilon_1 x_1^2)
\end{aligned} \tag{4}$$

Even though the equations given above are exact, in the sense that they do not involve any approximation and do not use the ε_i being small, their treatment still need further refining, and this will be done with the help of the method of averaging. Generally, the approach relies on studying the evolution equations for integrals of motion of the unperturbed system, i.e. in our case the normals to the planes of the large circles, with respect to the basic periodic solution of the latter. The averaging serves as a filter separating the main regular part of the solution from the oscillating one caused by small terms considered as perturbation, see [5].

We shall write the basic equation for the particle's motion on the sphere of unit radius in the form

$$\vec{x} = \cos(\omega t + \theta) \vec{e}_1 + \sin(\omega t + \theta) \vec{e}_2$$

vectors $\vec{e}_1, \vec{e}_2, \vec{e}_3$ determined by the equations:

$$\begin{aligned}
\vec{e}_1 &= \frac{1}{\sqrt{L_2^2 + L_3^2}} (0, L_3, -L_2) \\
\vec{e}_2 &= \frac{1}{L\sqrt{L_2^2 + L_3^2}} (-L_2^2 - L_3^2, L_1 L_2, L_1 L_3) \\
\vec{e}_3 &= \frac{1}{L} (L_1, L_2, L_3).
\end{aligned}$$

The angular velocity ω is given by the equation $\omega^2 = \dot{\vec{x}}^2 = L^2$, valid to within the first order of perturbation. Here L_1, L_2, L_3 are coordinates of the normal to the plane of the great circle determining the solution, i.e. the angular momentum.

Let us turn to the exact equations for the angular momentum (4). With the help of the equations given above and neglecting terms of the second, and higher, order in the ε_i , we can transform equations (4) in the form

$$\begin{aligned}
\dot{L}_1 &= \frac{2L^2 \varepsilon_2}{(L_2^2 + L_3^2)^2} \left[\cos(\omega t + \theta) L_3 + \sin(\omega t + \theta) \frac{L_1 L_2}{L} \right]^3 \left[\cos(\omega t + \theta) (-L_2) + \sin(\omega t + \theta) \frac{L_1 L_3}{L} \right] \\
&\quad - \frac{2L^2 \varepsilon_3}{(L_2^2 + L_3^2)^2} \left[\cos(\omega t + \theta) (-L_2) + \sin(\omega t + \theta) \frac{L_1 L_3}{L} \right]^3 \left[\cos(\omega t + \theta) L_3 + \sin(\omega t + \theta) \frac{L_1 L_2}{L} \right] \\
\dot{L}_2 &= \frac{2L^2 \varepsilon_3}{(L_2^2 + L_3^2)^2} \left[\cos(\omega t + \theta) (-L_2) + \sin(\omega t + \theta) \frac{L_1 L_3}{L} \right]^3 \left[\cos(\omega t + \theta) \cdot 0 + \sin(\omega t + \theta) \frac{-L_2^2 - L_3^2}{L} \right] \\
&\quad - \frac{2L^2 \varepsilon_1}{(L_2^2 + L_3^2)^2} \left[\cos(\omega t + \theta) \cdot 0 + \sin(\omega t + \theta) \frac{-L_2^2 - L_3^2}{L} \right]^3 \left[\cos(\omega t + \theta) (-L_2) + \sin(\omega t + \theta) \frac{L_1 L_3}{L} \right]
\end{aligned} \tag{5}$$

$$\begin{aligned} \dot{L}_3 &= \frac{2L^2\varepsilon_1}{(L_2^2 + L_3^2)^2} \left[\cos(\omega t + \theta) \cdot 0 + \sin(\omega t + \theta) \frac{-L_2^2 - L_3^2}{L} \right]^3 \left[\cos(\omega t + \theta)L_3 + \sin(\omega t + \theta) \frac{L_1L_2}{L} \right] \\ &\quad - \frac{2L^2\varepsilon_2}{(L_2^2 + L_3^2)^2} \left[\cos(\omega t + \theta)L_3 + \sin(\omega t + \theta) \frac{L_1L_2}{L} \right]^3 \left[\cos(\omega t + \theta) \cdot 0 + \sin(\omega t + \theta) \frac{-L_2^2 - L_3^2}{L} \right] \end{aligned}$$

It should be noted that the right-hand sides of Eqs.(5) comprise terms oscillating in time and terms that vary slowly. The situation can be treated within the framework of the averaging method, [5], that is on neglecting the oscillatory terms we obtain the averaged equations for the angular momentum

$$\begin{aligned} \dot{L}_1 &= \frac{3}{4} \frac{L_2L_3}{L^2} [(\varepsilon_3 - \varepsilon_2)L_1^2 + \varepsilon_3L_2^2 - \varepsilon_2L_3^2], \\ \dot{L}_2 &= \frac{3}{4} \frac{L_3L_1}{L^2} [-\varepsilon_3L_1^2 + (\varepsilon_1 - \varepsilon_3)L_2^2 + \varepsilon_1L_3^2], \\ \dot{L}_3 &= \frac{3}{4} \frac{L_1L_2}{L^2} [\varepsilon_2L_1^2 - \varepsilon_1L_2^2 + (\varepsilon_2 - \varepsilon_1)L_3^2]. \end{aligned} \tag{6}$$

It is worth noting that Eq.(6) have the Hamiltonian form determined by the usual Poisson brackets for the angular momentum, [6], [1],

$$\{L_i, L_j\} = \sum_k \varepsilon_{ijk} L_k,$$

and the Hamiltonian

$$H = \frac{3}{16} L^2 \sum_i \varepsilon_i \left[\left(\frac{L_i}{L} \right)^2 - 1 \right]^2. \tag{7}$$

This circumstance is particularly interesting because, usually, the averaging procedure is not compatible with Hamiltonian structure.

We may infer from the two integrals of motion, L^2 and H , that they admit of an explicit exact solution that can be cast in the form of the equation

$$t = \mp \frac{4}{3} (\varepsilon_2 + \varepsilon_3) L^2 \int \frac{dL_1}{\sqrt{D(\varepsilon_2L^2 - \varepsilon_3L_1^2 \mp \sqrt{D})(\varepsilon_3L^2 - \varepsilon_2L_1^2 \pm \sqrt{D})}}. \tag{8}$$

in which

$$D = -\varepsilon_1(\varepsilon_2 + \varepsilon_3)(L^2 - L_1^2)^2 - \varepsilon_2\varepsilon_3(L^2 + L_1^2)^2 + \frac{16}{3}(\varepsilon_2 + \varepsilon_3)L^2H.$$

The exact solution is not particularly practical. In this paper we shall not use it, but employ topological considerations and numerical simulation so as to understand the dynamics of \vec{L} and, consequently, the behaviour of geodetic coils. The important point is considering the stationary solutions to Eqs.(6) for which the right-hand sides turn out to be zero, and split into three parts S1, S2 and S3, determined by conditions on ε_i , as follows.

S1 No algebraic constraints imposed on ε_i :

- a. $L_{10} = 0, L_{20} = 0, L_{30} \neq 0;$
- b. $L_{10} = 0, L_{20} \neq 0, L_{30} = 0;$
- c. $L_{10} \neq 0, L_{20} = 0, L_{30} = 0;$

S2 The constraints on \vec{L} relaxed and linear constraints imposed on ε_i :

- a. $L_{10} = 0, L_{20} \neq 0, L_{30} \neq 0, \varepsilon_3 L_{20}^2 - \varepsilon_2 L_{30}^2 = 0$
- b. $L_{20} = 0, L_{30} \neq 0, L_{10} \neq 0, \varepsilon_1 L_{30}^2 - \varepsilon_3 L_{10}^2 = 0$
- c. $L_{30} = 0, L_{10} \neq 0, L_{20} \neq 0, \varepsilon_2 L_{10}^2 - \varepsilon_1 L_{20}^2 = 0$

S3 Vector \vec{L} subject to $L_{10} \neq 0, L_{20} \neq 0, L_{30} \neq 0$ and the quadratic constraints imposed on ε_i :

$$\frac{L_{10}^2}{\varepsilon_1 \varepsilon_2 - \varepsilon_2 \varepsilon_3 + \varepsilon_3 \varepsilon_1} = \frac{L_{10}^2}{\varepsilon_1 \varepsilon_2 + \varepsilon_2 \varepsilon_3 - \varepsilon_3 \varepsilon_1} = \frac{L_{10}^2}{-\varepsilon_1 \varepsilon_2 + \varepsilon_2 \varepsilon_3 + \varepsilon_3 \varepsilon_1}$$

It is worth noting that equations S2 involve the fulfilment of the inequalities $\varepsilon_2 \varepsilon_3 > 0, \varepsilon_3 \varepsilon_1 > 0,$ and $\varepsilon_1 \varepsilon_2 > 0$ for cases S2.a, S2.b, S2.c, respectively, whereas equations S3 involve

$$\begin{aligned} \varepsilon_1 \varepsilon_2 - \varepsilon_2 \varepsilon_3 + \varepsilon_3 \varepsilon_1 &> 0 \\ \varepsilon_1 \varepsilon_2 + \varepsilon_2 \varepsilon_3 - \varepsilon_3 \varepsilon_1 &> 0 \\ -\varepsilon_1 \varepsilon_2 + \varepsilon_2 \varepsilon_3 + \varepsilon_3 \varepsilon_1 &> 0 \end{aligned}$$

Linearizing Eqs.(6) at the stationary solutions and, considering small fluctuations of \vec{L} round them, we may study their stability, which turns out to be determined by the requirements

- S1
 - a. $\varepsilon_1 \varepsilon_2 > 0;$
 - b. $\varepsilon_2 \varepsilon_3 > 0;$
 - c. $\varepsilon_3 \varepsilon_1 > 0.$
- S2
 - a. $\varepsilon_1 \varepsilon_2 - \varepsilon_2 \varepsilon_3 + \varepsilon_3 \varepsilon_1 < 0;$
 - b. $\varepsilon_1 \varepsilon_2 + \varepsilon_2 \varepsilon_3 - \varepsilon_3 \varepsilon_1 < 0;$
 - c. $-\varepsilon_1 \varepsilon_2 + \varepsilon_2 \varepsilon_3 + \varepsilon_3 \varepsilon_1 < 0.$
- S3 any $\varepsilon_i.$

We may put these equations in a more graphic form using the integral $L^2 = const,$ and consider the motion of \vec{L} on a sphere of fixed radius, the integral of energy H taking appropriate values. Then the stable solutions are fixed points as regards Eqs.(6), the stable and the unstable points are foci and saddle points, respectfully, the separaterixes being lines joining the fixed points. Together, they generate a graph on the sphere, having the fixed points as vertices and the separaterixes as edges. It is important that the separaterixes, i.e. the edges of the graph, are oriented according to the time, $t,$ so that the graph is the oriented one, and invariant with respect to the symmetry $\vec{R} \rightarrow -\vec{R}, t \rightarrow -t.$

The pictures of the separatrixe net on the sphere are rather difficult for visualizing, and therefore there is a need for some means which are easier to implement. We shall employ the familiar construction of the projective plane, which runs as follows. Given a pair of twin points \vec{R} and $-\vec{R}$ belonging to the sphere we shall choose the representative of the pair determined by the condition $R_3 \geq 0;$ this enables us to consider only the upper part of the sphere. Next take the projection of the upper hemi-sphere on x-y plane along axes-z. Thus, a pair of antipodal twins obtains a representative in the disk, i.e. a point inside the disk or a pair of antipodal points at the boundary. The separatrixe nets constructed in this way on the projective plain, are shown in FIGs(4 — 7). It is important that the equations of motion are invariant under the transformations $P_i, \quad i = 1, 2, 3$

$$P_i : \quad t \rightarrow -t, \quad L_i \rightarrow -L_i \tag{9}$$

which generate automorphisms of the graph.

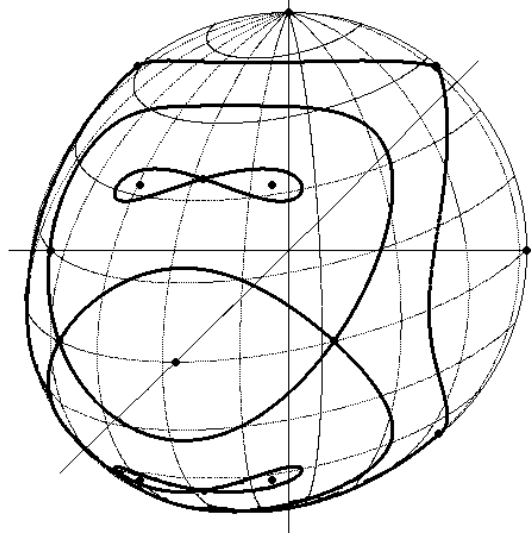


FIG. 4: Separatrix net corresponding to the graph of Type I on the sphere; the twin points correspond to the symmetry given by Eq.(9)

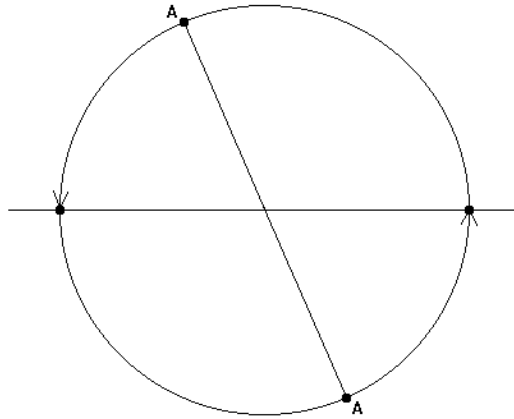


FIG. 5: Diagramme of the projective plain by means of a disk with identified antipodal points at the boundary circle.

From the fact that the transformation

$$P : \quad t \rightarrow -t, \quad L_i \rightarrow -L_i, \quad i = 1, 2, 3, \quad P = P_1 P_2 P_3 \quad (10)$$

leaves Eqs.(6) invariant, we infer that a point belonging to a solution of Eqs.(6) has its counterpart, or twin, at the antipodal point and therefore one may visualize the dynamics of \vec{L} on a sphere with identified antipodal points, that is the projective plane.

Now we are in a position to determine the topological types of the graphs by employing the computer simulation of the Eqs.(6) in conjunction with the knowledge of the topological types of the fixed points obtained above. It should be noted that we must check as to whether the solutions provided by Eqs.(6) agree with those given by original Eqs.(1), see FIG.(10). The phase picture can be obtained by constructing a mesh generated by solutions to Eqs.(6), taking into account the types of fixed points. The results are illustrated in FIGs(4 — 7).

We obtain the following topological types of the graphs:

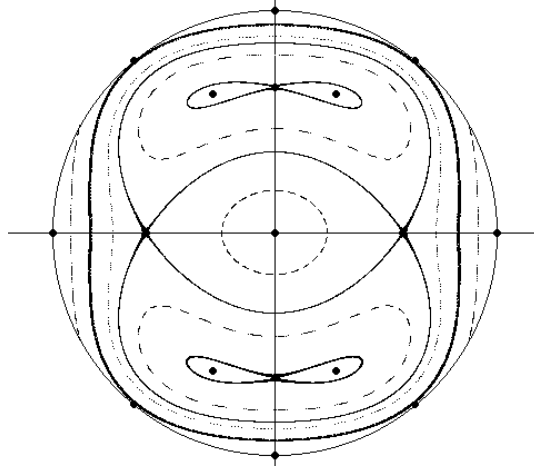


FIG. 6: Type I trajectories of the auxiliary system on projective plain; dashed lines are typical trajectories, the solid ones separatrixes. Parameters of deformation: $\varepsilon_1 = 0.02$, $\varepsilon_2 = 0.03$, $\varepsilon_3 = 0.04$.

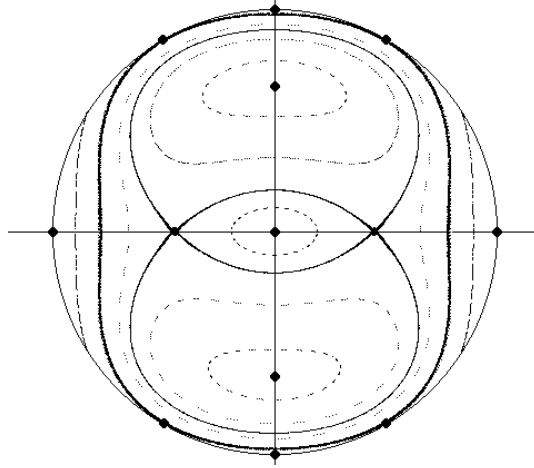


FIG. 7: Type II trajectories of the auxiliary system on the projective plain; dashed lines are typical trajectories, the solid ones separatrixes. Parameters of deformation: $\varepsilon_1 = 0.01$, $\varepsilon_2 = 0.03$, $\varepsilon_3 = 0.04$.

Type I FIG.4, 7 foci and 6 saddles; ε_i being subject to the constraints:

$$\begin{aligned} \varepsilon_1\varepsilon_2 - \varepsilon_2\varepsilon_3 + \varepsilon_3\varepsilon_1 &> 0 \\ \varepsilon_1\varepsilon_2 + \varepsilon_2\varepsilon_3 - \varepsilon_3\varepsilon_1 &> 0 . \\ -\varepsilon_1\varepsilon_2 + \varepsilon_2\varepsilon_3 + \varepsilon_3\varepsilon_1 &> 0 \end{aligned} \quad (11)$$

Type II FIG.5, 5 foci and 4 saddle points; ε_i are not equal to zero, have the same sign, and at least one of eqs.(11) is not true.

Type III FIG.6, 3 foci and 2 saddle points; ε_i being subject to one of the following constraints: $\varepsilon_2\varepsilon_3 > 0$ and $\varepsilon_1\varepsilon_2 \leq 0$; $\varepsilon_3\varepsilon_1 > 0$ and $\varepsilon_2\varepsilon_3 \leq 0$; $\varepsilon_1\varepsilon_2 > 0$ and $\varepsilon_3\varepsilon_1 \leq 0$.

Type IV FIG.7, 2 foci and 1 saddle point; ε_i being subject to one of the following constraints: $\varepsilon_1 = 0$ and $\varepsilon_2\varepsilon_3 \leq 0$; $\varepsilon_2 = 0$ and $\varepsilon_3\varepsilon_1 \leq 0$; $\varepsilon_3 = 0$ and $\varepsilon_1\varepsilon_2 \leq 0$.

The topological types of the separatrix nets depend on values of the coefficients of the deformation ε_i , and generate regions I, II, III, IV in the ε_i space. Taking into account the homogeneous form of the constraints imposed on ε_i , we may visualize them on the projective plane corresponding to ε_i , see FIG.9.

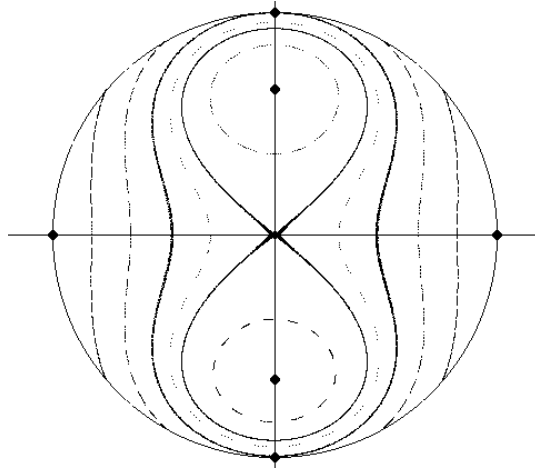


FIG. 8: Type III trajectories of the auxiliary system on the projective plain; dashed lines are typical trajectories, the solid ones separatrixes. Parameters of deformation: $\varepsilon_1 = -0.02$, $\varepsilon_2 = 0.03$, $\varepsilon_3 = 0.04$.

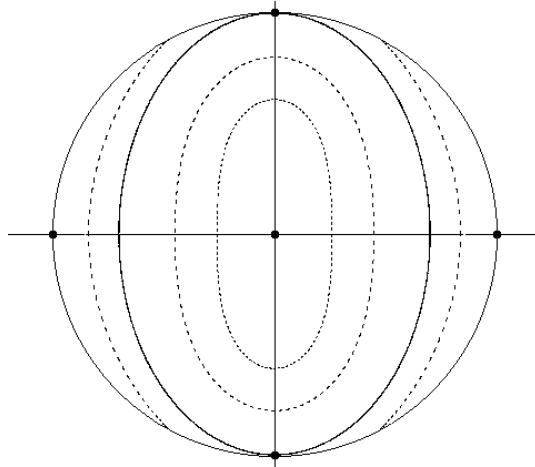


FIG. 9: Type IV trajectories of the auxiliary system on the projective plain; dashed lines are typical trajectories, the solid ones separatrixes. Parameters of deformation: $\varepsilon_1 = -0.01$, $\varepsilon_2 = 0.00$, $\varepsilon_3 = 0.01$.

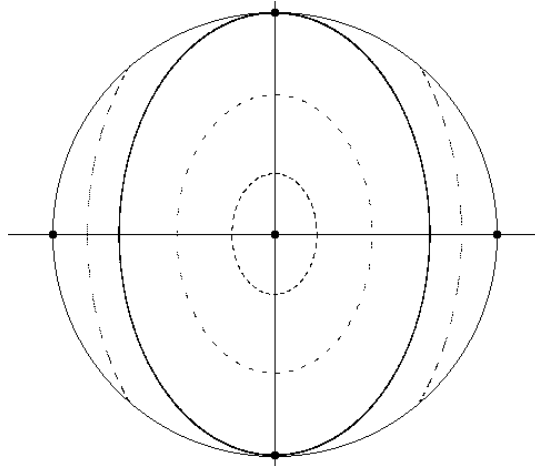


FIG. 10: Ellipsoid with the main axes: 1.01, 1.02, 1.03; dashed lines are typical trajectories, the solid separatrixes.

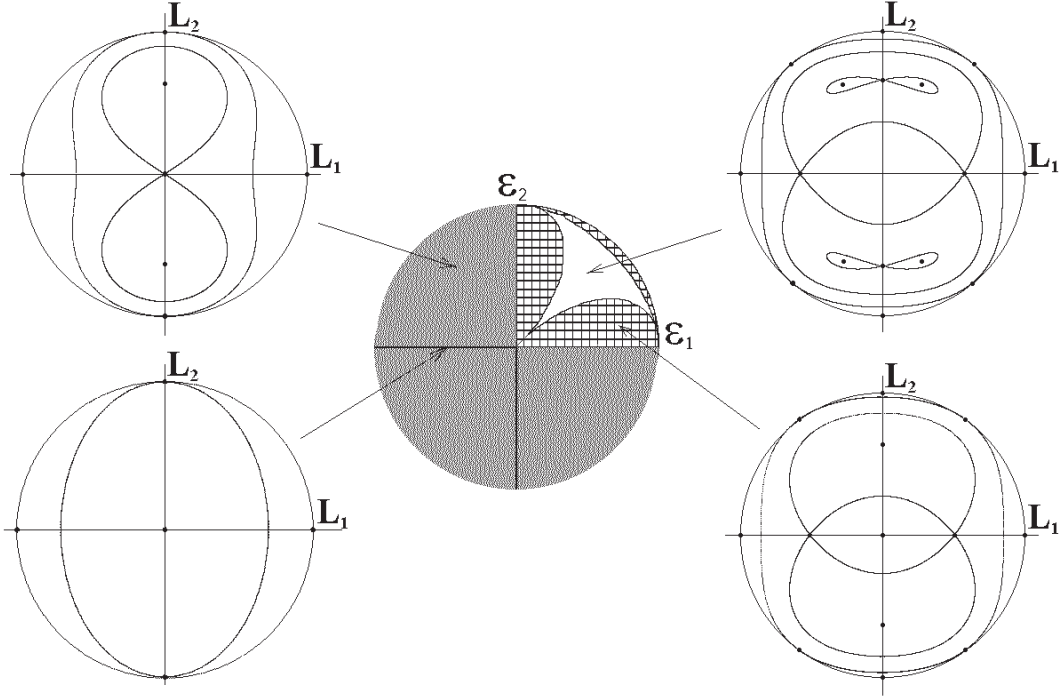


FIG. 11: Regions of ε_i corresponding to Types I - IV of the solutions to the auxiliary system, indicated on the projective plain represented by a disk with identified antipodal points at the boundary. The white area indicates Type I solutions, the filled and the barred ones Type II and Type III. The lines dividing the Type I and Type II regions are subject to Eq.(12)

It is important that the lines dividing the domains corresponding to types I and II, FIG.11, are given by the homogeneous equations

1. $\varepsilon_1\varepsilon_2 - \varepsilon_2\varepsilon_3 + \varepsilon_3\varepsilon_1 = 0$
2. $\varepsilon_1\varepsilon_2 + \varepsilon_2\varepsilon_3 - \varepsilon_3\varepsilon_1 = 0$
3. $-\varepsilon_1\varepsilon_2 + \varepsilon_2\varepsilon_3 + \varepsilon_3\varepsilon_1 = 0$

(12)

Each equation determines a projective circle on the projective plane of the homogeneous variables $\varepsilon_1, \varepsilon_2, \varepsilon_3$, see FIGs.14.

It is important that the solutions to Eqs.(6) have the specific feature that the topological type of the graph is completely determined by the numbers of foci and saddle points. The dependence of the conformations of the foci and the saddles on values of ε_i is illustrated in FIG.9.

We see that the topological types of the graphs are non-trivial enough, and the graphs realized on the sphere differ from those on the projective plain. This circumstance is due to the fact that the graphs on the projective plain are obtained from those on the sphere by factoring with transformation (10), see FIG.13.

III. CONCLUSION

The key point of the present investigation is the concept of geodetic coil which enables us to cast intuitive geometric ideas in analytical form, and relies on constructing an auxiliary hamiltonian system, which can be considered as a reduction of the initial problem to that of constructing a graph on projective plane. In analytical terms, one may consider it as an asymptotic reduction of the system of equations for geodesics on a deformed sphere to the system

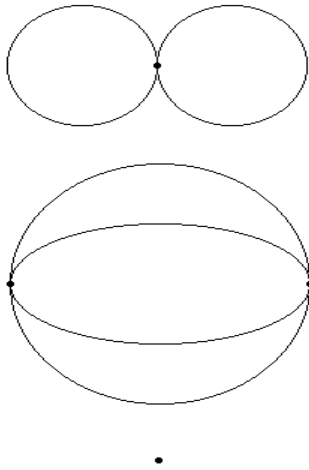


FIG. 12: Topological types of the separatrix nets; Type I — IV.

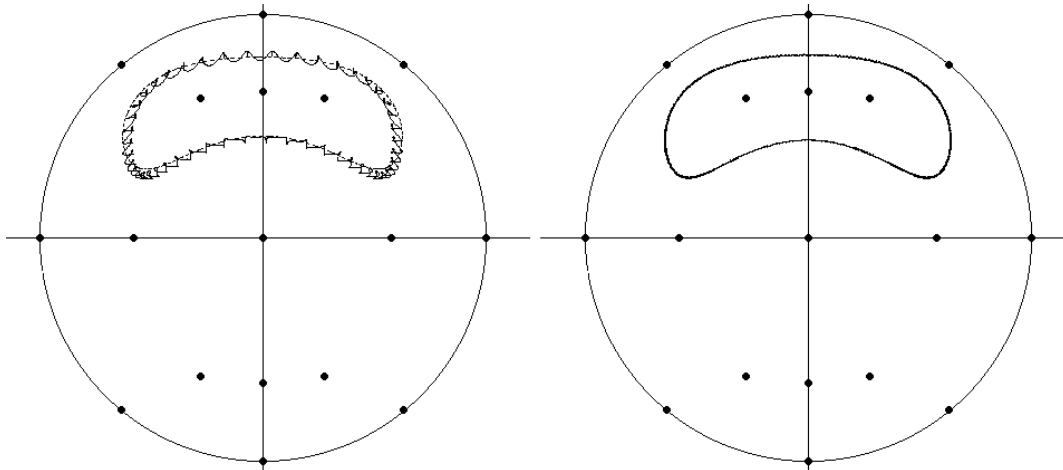


FIG. 13: Comparison of the solution to: A. the initial equations for geodesics; B. the averaged equation given by the auxiliary system.

similar to that of the top, with the hamiltonian of the fourth order. The simplification we get in this way, is substantial. Indeed, the Hamiltonian system for geodesics could be non-integrable, whereas the auxiliary system is totally integrable, and its phase space can be described by a graph that comprises vertices, which correspond to stationary solutions, or almost closed geodesics, and edges, which can be visualized as geodetic coils joining them. The important thing is that the arguments, of purely analytical and topological nature, which this analysis involves, turn out to be helpful for the numerical simulation of the equations for geodetic lines, which admits us to give a tangible realization of the visualization problem for geodesics on a surface.

In fact, this paper is profoundly motivated by the technical means provided by numerical modelling, which has allowed us to obtain the final picture of the problem's phase space in terms of the separatrix graphs. Thus, we feel that the approach used in this paper is the symbiosis of the methods of analytical mechanics, computer analysis, and topology. The latter is particularly important, giving the conceptual structure for the problem of geodetic lines on the deformed sphere. At this point it should be noted that the detailed picture of the phase space reconstruction should provide a description of imbedding the invariant torii, which could exist in some regimes, and, perhaps, the domains

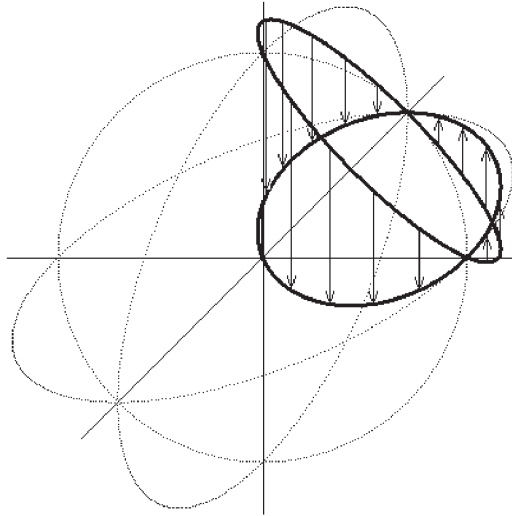


FIG. 14: Intersection of the conic determining the boundary line of **Type I** and the sphere. The projection on the disk gives the representation of the line on the projective plain.

of chaotic dynamics, peculiar for non-integrable problems, [7].

The solution obtained in this paper for the geodesics on the deformed sphere does not preclude the chaotic regimes of geodesic lines, even though the auxiliary hamiltonian system turns out to be completely integrable. It is worth noting that the dynamics of geodesics gives a graphic example of the chaos in riemannian geometry, [7]. This set of important problems, lying at the border between nonlinear mechanics, and riemannian geometry and topology, deserves further studying.

Acknowledgment

The authors are thankful to A.T.Fomenko, A.V.Bolsinov, and Yu.S.Volkov for the useful discussions.

This work was supported by the grants NS - 1988.2003.1, and RFFI 01-01-00583, 03-02-16173, 04-04-49645.

-
- [1] V.I.Arnold, *Mathematical Methods in Classical Mechanics*, Ch.9, Springer-Verlag, New York (1992).
 - [2] S.P.Novikov, B.A.Dubrovin, and A.T.Fomenko, *Modern Geometry*, Springer-Verlag, New York (1984).
 - [3] C.G.J Jacobi, *Vorlesungen über Dynamik*, Ch.28, URSS, Moscow (2004).
 - [4] Yu.S.Volkov, *Geodesics on torii*, unpublished.
 - [5] R.W.Hamming, *Numerical Methods for Scientists and Engineers*, Ch.24, McGraw-Hill, New York (1962).
 - [6] E.J.Routh, *Dynamics of a System of Rigid Bodies*, Ch.10, London - New York, Macmillan (1891 - 92).
 - [7] A.V.Bolsinov and A.T.Fomenko, *Integrable Hamiltonian Systems*, Ch. 14, Chapman and Hall, Roca Raton (2004).